AWARD NUMBER: W81XWH-19-1-0475

TITLE: Biofabrication of Cell-Decorated Telocollagen Fibers of Extraordinary Strength for Regenerative Tendon and Myotendinous Junction Repair

PRINCIPAL INVESTIGATOR: Dr. Michael Francis

CONTRACTING ORGANIZATION: Embody LLC

REPORT DATE: August 2020

TYPE OF REPORT: Annual

PREPARED FOR: U.S. Army Medical Research and Materiel Command
Fort Detrick, Maryland 21702-5012

REPORT DOCUMENTATION PAGE

Form Approved
OMB No. 0704-0188

1. REPORT DATE	**2. REPORT TYPE**	**3. DATES COVERED**
August 2020	Annual Technical Report	15 July 2019 – 14 July 2020

4. TITLE AND SUBTITLE
Biofabrication of Cell-Decorated Telocollagen Fibers of Extraordinary Strength for Regenerative Tendon and Myotendinous Junction Repair

5a. CONTRACT NUMBER

5b. GRANT NUMBER
W81XWH-19-1-0475

5c. PROGRAM ELEMENT NUMBER

6. AUTHOR(S)
Michael Francis, PhD*, Kyle Christensen, PhD, Yas Maghdouri-White, PhD, Nardos Sori, PhD

*Corresponding author E-Mail: mfrancis@embody-inc.com

5d. PROJECT NUMBER
0011332768

5e. TASK NUMBER

5f. WORK UNIT NUMBER

7. PERFORMING ORGANIZATION NAME(S) AND ADDRESS(ES)
EMBODY, INC.
JEFFREY CONROY
4111 MONARCH WAY STE 409
NORFOLK VA 23508-2563

8. PERFORMING ORGANIZATION REPORT NUMBER

9. SPONSORING / MONITORING AGENCY NAME(S) AND ADDRESS(ES)
U.S. Army Medical Research and Development Command
Fort Detrick, Maryland 21702-5012

10. SPONSOR/MONITOR'S ACRONYM(S)
USAMRDC

11. SPONSOR/MONITOR'S REPORT NUMBER(S)

12. DISTRIBUTION / AVAILABILITY STATEMENT
Approved for Public Release; Distribution Unlimited

13. SUPPLEMENTARY NOTES

14. ABSTRACT
Musculoskeletal tissue injuries, including those occurring at the myotendinous junction (MTJ), are the leading cause for medical encounters for warfighters. Nonsurgical treatments and leading clinical repair scaffolds have significant limitations. To address this need, we developed a novel biomanufacturing, or 3D bioprinting, approach to produce strong, cellularized, living biomimetic grafts. Our bioprinting process utilizes strong clinical grade collagen microfibers and was optimized to controllably produce grafts with designed geometries and cellular distributions throughout. Printed grafts offer excellent biocompatibility, functional architectures, high cell viability, and mechanical properties mimicking those of native tendon. In all, this technology greatly outperforms previously developed tissue engineering approaches for producing biomimetic grafts with potential to improve the repair and regeneration of musculoskeletal and MTJ tissue injuries.

15. SUBJECT TERMS
Collagen, additive manufacturing, biomanufacturing, bioprinting, microfiber, biomimicry, myotendinous junction

16. SECURITY CLASSIFICATION OF:			**17. LIMITATION OF ABSTRACT**	**18. NUMBER OF PAGES**	**19a. NAME OF RESPONSIBLE PERSON**
a. REPORT	**b. ABSTRACT**	**c. THIS PAGE**			**19b. TELEPHONE NUMBER** *(include area code)*
Unclassified	Unclassified	Unclassified	Unclassified	20	USAMRMC

Standard Form 298 (Rev. 8-98)
Prescribed by ANSI Std. Z39.18

TABLE OF CONTENTS

1. INTRODUCTION:

Musculoskeletal tissue injuries, including those at the myotendinous junction (MTJ), are the leading cause for all medical encounters for warfighters at ~2 million cases per year, with extremity injuries accounting for up to 79% of trauma cases in theater. Available therapies have significant limitations, such that various tissue engineering approaches have been explored for the on-demand fabrication of living grafts for the treatment of these injuries. However, recreating the structural, biochemical, and mechanical likeness of native tissue in an automated, scalable fabrication process has remained a challenge. Addressing these shortcomings, a novel biomanufacturing process was developed herein as a versatile and capable approach to produce therapeutic grafts with the potential to treat tendon/ligament and MTJ-related injuries. Produced grafts were assessed for their geometric fidelity, biocompatibility, cellularity, and mechanical properties and were found to mimic key aspects of native musculoskeletal tissue. It's envisioned that this platform biomanufacturing technology can produce cellularized grafts which promote regeneration and functional recovery in debilitating musculoskeletal tissue injuries.

2. KEYWORDS:

Collagen, additive manufacturing, biomanufacturing, bioprinting, microfiber, biomimicry, myotendinous junction

3. ACCOMPLISHMENTS:

What were the major goals of the project?

Objective 1: Bioprinting of strong and stable collagen microfibers decorated with viable cells

Major Task 1: Design, build and test robust printheads for controllable high-output cell decorated collagen fiber grafts to mimic native tendon tissue strength and cellular arrangement.

Subtask 1: Design custom printhead to fit our commercial Folger Tech FT-5 R2 Large Scale 3D Printer.

Timeline (month of project): 1-4.
Percent completion: 100%

Subtask 2: Regulatory approvals for the use of human mesenchymal stem cells (hMSCs) (RoosterBio) by HRPO.

Timeline (month of project): 1-3.
Percent completion: 100%

Subtask 3: Generate sterile, crosslinked collagen fibers and culture research grade hMSCs (RoosterBio) for use in the 3D bioprinter.

Timeline (month of project): 4
Percent completion: 100%

Subtask 4: Create test scaffolds by feeding collagen fibers through the printhead, into the seeding reservoir with research grade MSCs (RoosterBio) and onto the build space.
Timeline (month of project): 5-8.
Percent completion: 100%

Subtask 5: Assess test scaffolds for cell distribution, viability and mechanical strength
Timeline (month of project): 9.
Percent completion: 100%

Subtask 6: Optimize process parameters (flow and draw rates, cell density and hyaluronic acid concentration) for optimal cell decoration on fibers using sterilized microfluidic collagen fibers and clinical grade MSCs (RoosterBio).
Timeline (month of project): 10-11
Percent completion: 100%

Subtask 7: Build repeating benchmark scaffolds using collagen fibers and MSCs to create test articles for 3D bioprinter performance validation.
Timeline (month of project): 11
Percent completion: 100%

Subtask 8: Finalize performance validation by testing benchmark scaffolds for cell distribution and viability, cellular metabolic activity and strength.
Timeline (month of project): 12
Percent completion: 100%

Subtask 9: IACUC and ACURO approval
Timeline (month of project): 4-9.
Percent completion: 100%

What was accomplished under these goals?

1) *Major activities*

Designed, manufactured, and tested a novel custom three-dimensional (3D) biomanufacturing, or bioprinting, apparatus to interface with commercial Folger Tech FT-5 R2 large scale 3D printer.

Generated sterile, crosslinked collagen microfibers and cultured research grade human mesenchymal stem cells (hMSCs) (RoosterBio) for use with the 3D bioprinting approach.

Optimized printing process conditions and produced cellularized scaffolds from collagen fiber and hMSCs for process validation. Assessed scaffolds for cell viability, distribution, and mechanical strength.

2) *Specific objectives*

Developed a novel additive manufacturing approach to produce cellularized scaffolds consisting of dense, highly aligned, strong collagen microfibers. Specifically, collagen microfibers were robotically coated with cells in suspension and wrapped around a rigid frame in designed 3D patterns. In mimicking native ligament and tendon ultrastructure, these cell-coated fibers were wrapped in parallel next to and on top of themselves to form rectangular macrostructures of designed width, length, and thickness.

Strong, stable microfibers were produced from clinical-grade collagen using our previously developed microfluidic extrusion platform. These crosslinked microfibers were produced in significant quantity, sterilized using electron beam sterilization, and supplied as a feed material for our 3D bioprinting process. For the fabrication of cellularized scaffolds, research grade hMSCs were obtained from RoosterBio and cultured for use in our 3D bioprinting process.

Utilized our novel additive biofabrication process to produce cellularized scaffolds from collagen microfiber and hMSCs with varying geometries. Printing process conditions were optimized and scaffolds were assessed for cell viability and distributions throughout scaffolds using microscopic imaging with fluorescent and live/dead labeling of cells. Scaffold mechanical properties including ultimate tensile stress (UTS) and tangent modulus were assessed using uniaxial tensile testing.

3) *Significant results*

1. Concept and design

We developed a novel additive biofabrication approach deemed cell-decorated collagen (CDC) fabrication to produce cellularized scaffolds consisting of dense, highly aligned, strong collagen microfiber. Specifically, collagen microfiber is coated with a cell suspension and robotically wrapped around a rigid frame. In mimicking native ligament and tendon ultrastructure, this cell-coated fiber is wrapped in parallel next to and on top of itself to form rectangular macrostructures of designed width, length, and thickness. This results three-dimensional (3D) structures consisting of layers of densely packed parallel collagen fiber with cells seeded uniformly throughout. Scaffolds are cultured on custom rigid frames with varying geometries to maintain the macroscopic shape and orientation of the fiber before removal. The use of these scaffolds aims to promote regeneration and recovery of function in musculoskeletal tissue injuries and the myotendinous junction in particular.

To enable CDC fabrication, a custom extrusion printhead (**Figure 1A**) was designed and mounted to a Folger Tech FT-5 R2 commercial 3D printer. Two separate planetary geared stepper motors with lead screw assemblies mechanically compress disposable syringes individually, extruding cell suspension with sub-microliter resolution. While a single cell suspension is printed at a time herein, the dual-solution printhead will prospectively facilitate the production of heterogeneous scaffolds with differing cell populations in distinct regions.

During printing, cell suspension is extruded into the seeding manifold, where it builds up in a small coating reservoir (**Figure 1B**). Collagen microfiber was produced using a wetspinning process, desiccated, wound onto custom spools, and sterilized by electron beam sterilization prior to printing. Up to 3 spools of collagen microfiber are utilized during printing, each of which is fed through the seeding manifold. Within the seeding manifold, the collagen fiber is uniformly coated by the extruded cell suspension. The volume of cell suspension extruded per millimeter of drawn fiber is a user-determined process parameter and offers a means to control the resulting cell density and total number of cells throughout a scaffold.

A custom collection assembly was designed (**Figure 1A**) in which small rigid frames (**Figure 1C**) are held between two stepper motors. Typically, frame designs consist of two horizontal bars or dowels held a fixed distance apart by custom 3D-printed frame ends, forming a central opening to limit the effects of cell migration from the scaffold to the frame and additionally enable improved nutrient diffusion to the scaffold from surround cell culture media. A number of frame geometries have been utilized depending on the desired functional aspects, such as facilitating production of multiple scaffolds or larger scaffolds, securing loose fiber ends from the beginning and end of printed scaffolds, or allowing straightforward handling and removal of scaffolds from the frames. Stepper motors driving the frame rotation are mounted on manual linear stages which allow for straightforward loading and removal of frames between consecutive prints.

Prior to printing, fiber is fed through the seeding manifold and attached at an initial anchoring point on the collection assembly. As the frame is rotated by the motors, fiber is drawn under tension through the seeding manifold and coated by the extruded cell suspension. By coordinating the rotation of the frame and linear translation of the printhead along the width of the frame (the feed), cellularized scaffolds of dense, highly aligned collagen microfiber are produced.

A custom Python code was developed to accept user inputs for designed scaffold geometry and printing parameters, number of scaffolds per frame, scaffold width, height, number of layers of fiber, extruded volume of cell suspension per millimeter drawn fiber, feed distance between parallel fibers, and frame rotation rate, and output a corresponding g-code file. The g-code file contains all parameters and motion/extrusion commands to execute a designed print, and is sent to the printer to produce the designed scaffold.

To print cellularized scaffolds, cells are suspended in a hyaluronic acid (HA) solution prepared in Dulbecco's Modified Eagles Medium (DMEM) or a cell-type specific culture media. Hyaluronic acid is a key component of the extracellular matrix and is utilized herein as a "cellular glue" to facilitate the adherence of cells to collagen microfiber. Culture media provides the necessary nutrients and cytocompatible environment to sustain cell health during printing.

Printing process parameters were optimized to facilitate consistent and controlled fabrication. HA concentrations ranging from 2.5 mg/mL to 10 mg/mL were tested for handleability and printability. It was found that an optimal concentration of 5 mg/mL could be accurately pipetted and extruded, readily filtered using a 0.2 um filter for sterilization, provided sufficient viscosity to limit cell settling during printing, and facilitated uniform coating of collagen fiber with cell suspensions. An extrusion rate of 0.38 uL per 10 mm of drawn fiber was found to result in uniform coating of fiber. A feed distance between adjacent fiber strands of 0.15 mm was found to be optimal and could be varied to control scaffold porosity. A frame rotation rate of 10 rpm was used to produce scaffolds quickly and did not appear to affect cell health due to fluid shear stresses.

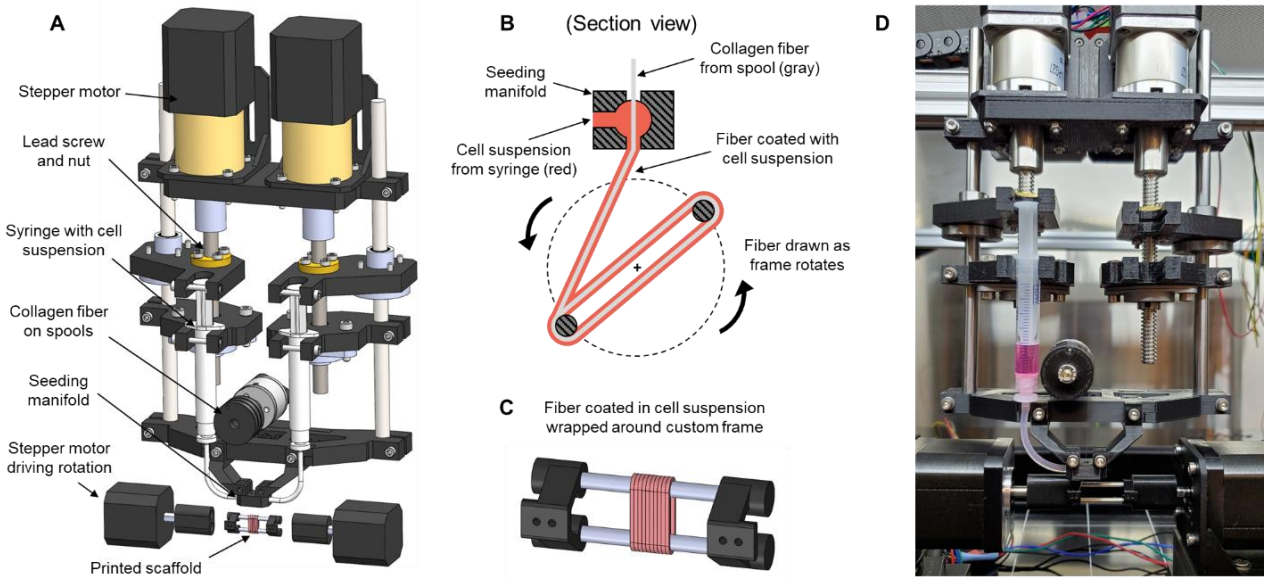

Figure 1. Cell-decorated collagen fabrication system design. (A) CAD model of custom extrusion printhead and frame assembly with key components identified. (B) Section view illustrating the cell seeding and scaffold biofabrication process. Collagen fiber passes through a seeding manifold, where it is uniformly coated with a cell suspension. The coated fiber is drawn onto a frame of arbitrary shape and dimensions and wrapped in parallel and on top of itself to form a scaffold. (C) Enlarged CAD model of parallel fiber scaffold wrapped around a rigid frame with a multifunctional design. (D) Photograph of printhead and frame assembly during printing.

2. Assessment of bioprinting fidelity

Cellularized collagen microfiber scaffolds were printed rapidly and repeatably onto various frame geometries (**Figure 2A, B, C**). Multiple scaffolds were printed onto frames consisting of two steel dowels held together by 3D-printed PLA frame ends and secured into individual bundles by tying knots at each end using suture (**Figure 2A**). Custom PLA frames were used to print larger scaffolds (**Figure 2B**) and frame geometries can be easily modified for producing millimeter to centimeter scale scaffolds. Specialized frame geometries were used to print scaffolds directly onto and between two lengths of suture and maintain tension on scaffolds during culture (**Figure 2C**). After securing scaffolds into bundles using suture, they can be easily removed from the frames (**Figure 2D**) by removing one or both PLA frame ends and sliding scaffolds off of the steel dowels, for example. Regardless of custom geometry, rigid frames were found to maintain fiber alignment and macrostructure of printed scaffolds in culture over several weeks.

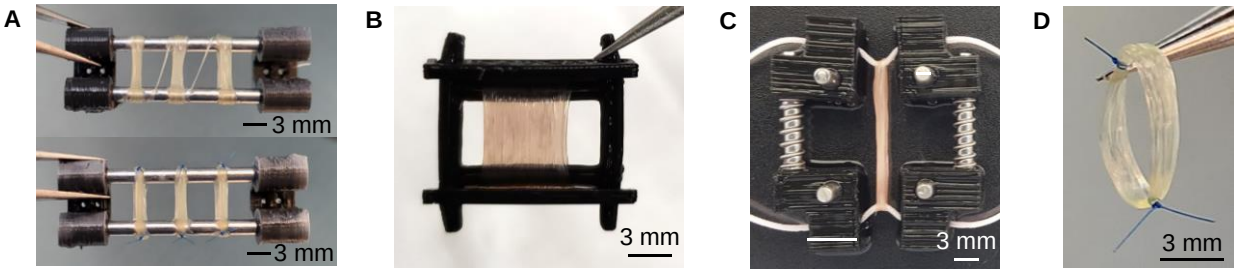

Figure 2. Printed test scaffolds with varying scaffold and frame geometries. (A) Three printed scaffolds on a multifunctional frame before (top) and after (bottom) being secured with suture. (B) A larger printed scaffold on another custom frame geometry. (C) A scaffold printed onto two lengths of suture and held in tension by a custom frame. (D) A printed scaffold held by tweezers after being secured with suture and removed from a frame.

Transmitted light microscopy of printed scaffolds shows striations indicative of densely packed parallel fiber after 4 days of culture (**Figure 3A**). Fluorescence imaging of hMSCs stained with the cytoplasmic label DiD (green), dead cell nuclear label EthD-1 (red), and fiber autofluorescence at 405 nm (blue) shows scaffolds after 4 days of culture with cells distributed throughout the scaffold (**Figure 3B**). Notably, cells are elongated parallel to the fiber direction as is typical for native tendon and ligament tissue. Images such as this were taken throughout varying fields of view and in different planes throughout scaffolds as a qualitative means to assess cell distributions. Immediately after printing, cells were observed to have a largely uniform distribution throughout scaffolds, with no observable localizations of comparatively high or low density. Similarly, cells maintained a largely uniform distribution during culture as they proliferated and eventually became confluent throughout printed scaffolds. Cell suspensions ranging from 1×10^6 to 6×10^6 cells/mL were successfully printed, with optimal concentrations chosen based on the desired resulting graft cell density.

As a means to assess the fundamental consistency of the printing process, a single grouping of three collagen microfiber strands (printed simultaneously from 3 spools of fiber attached to the printhead) was printed with hMSCs and cells were labeled with the same fluorescent stains after 4 days of culture (**Figure 3C**). These three fiber strands act as the "building blocks" of printed scaffolds, as three fiber strands are continuously drawn through the printhead, seeded with cells, and wrapped next to and on top of one another to form 3D scaffolds. The uniformity of cells on these three "building block" strands is indicative of a consistent fundamental cell seeding process, such that resulting scaffolds are expected to have consistent cellularity throughout, regardless of overall scaffold dimensions or geometry.

Cell viability throughout printed scaffolds was assessed both qualitatively and quantitatively by fluorescent imaging of hMSCs stained with the cytoplasmic label DiD and dead cell nuclear label EthD-1. Qualitatively, a generally high viability is indicated by live cells (green) greatly outnumbering dead cells (red) (**Figure 3B, C**). Quantitatively, ImageJ was used with established particle counting approaches to compare the number of live and dead cells throughout scaffolds immediately after printing. Across various scaffold geometries and printing conditions, cell viability was found to remain consistently above 80%. For representative grafts printed with typical process parameters, hMSCs were found to be 93.2±1.7% (standard deviation, n=6) viable immediately after printing. Over extended culture periods, quantifying cell viability by fluorescent imaging becomes difficult as cells become confluent throughout the scaffolds with individual cells becoming essentially indistinguishable (**Figure 4A**). Qualitatively, it was observed that cells maintain a very high viability during extended periods of culture, with live cell numbers estimated to be in the tens of thousands greatly outnumbering dead cells.

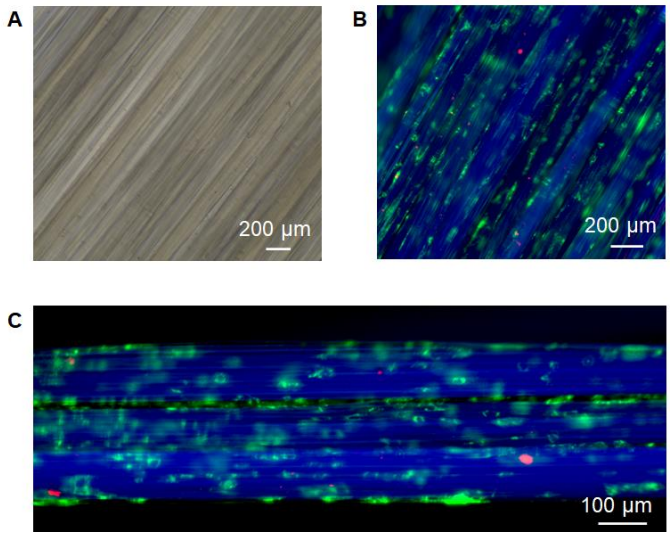

Figure 3. Microscopic imaging of printed scaffolds. Fluorescence images show all cells with the cytoplasmic label DiD (green), dead cell nuclei label EthD-1 (red), and collagen fiber autofluorescence at 405 nm (blue). (A) Transmitted light image of a printed scaffold showing striations indicative of densely packed parallel fiber after 4 days of culture. (B) Fluorescence image showing hMSCs uniformly distributed throughout and elongated parallel to the fiber direction after 4 days of culture. (C) Fluorescence image showing hMSCs attached to and distributed along three strands of collagen fiber after 4 days in culture.

Benchmark scaffolds were printed with hMSCs suspended at 4×10^6 cells/mL to assess cell metabolic activity over time using the alamarBlue assay. Scaffolds (n=6) were incubated for 6 hours in 10% alamarBlue solution in hMSC growth media and fluorescence was measured after 1, 4, and 7 days in culture according to standard assay protocols (**Figure 4B**). Metabolic activity of cellularized scaffolds in culture was found to increase 5-fold over 7 days of culture, indicating an increase in cell health, activity, and proliferation.

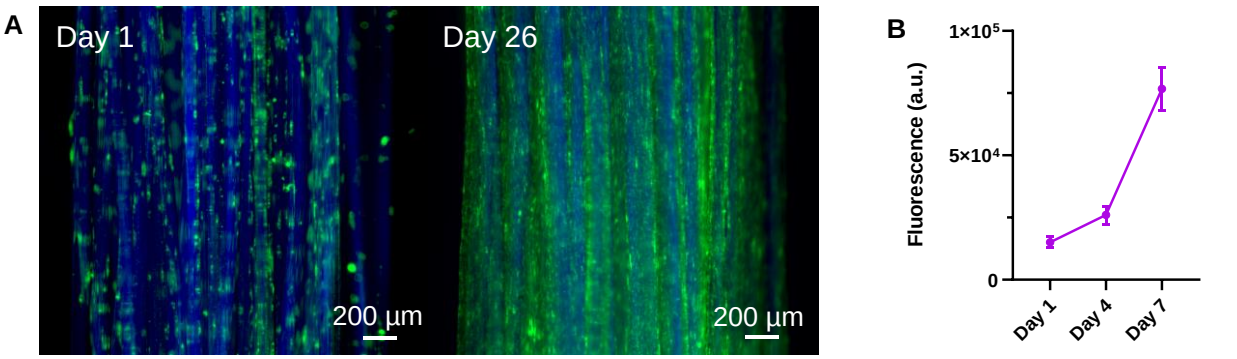

Figure 4. Cell proliferation and metabolic activity. Fluorescence images show all cells with the cytoplasmic label DiD (green) and collagen fiber autofluorescence at 405 nm (blue). (A) Fluorescence images of printed scaffolds showing a largely uniform initial distribution of cells after 1 day of culture and a confluent densely-cellularized scaffold after 26 days of culture. (B) Fluorescence indicating an increase in cell metabolic activity using the alamarBlue assay for scaffolds printed with human tenocytes after 1, 3, and 7 days of culture. Error bars represent standard error of measurement.

3. Assessment of cellular distribution and uniformity

The uniformity of cells distributed throughout scaffolds was quantified by adapting a method for analyzing the distribution of particles in a field of view using Shannon entropy. This approach offers a means to validate the bioprinting process control and repeatability, and may be applied to various tissue engineering approaches which have traditionally relied on subjective and qualitative descriptions. In a typical 2 mm × 2 mm field of view of a printed scaffold, rat muscle progenitor cells (rMPCs) were stained and imaged with the cytoplasmic label DiD (green) after 14 days in culture with fiber autofluorescence at 405 nm (blue) (**Figure 5A**). The image was converted to binary, such that cells are shown in black on a white background (**Figure 5D**). Image analysis was then used to measure the average grayscale value, with white pixels measured as 0 and black pixels measured as 255, of pixel columns taken across the 2 mm transverse direction, with the value for each column being the average grayscale value of pixels contained in that column. Similarly, the grayscale value is measured for pixel rows taken along the longitudinal direction with the value for each row being the average grayscale value of pixels contained in that row. These measured grayscale values were then grouped into 100 bins and normalized to the total grayscale value of the field of view to represent the relative cellularity. This relative cellularity is plotted across the transverse (**Figure 5E**) and longitudinal (**Figure 5F**) directions.

Plotting the relative cellularity measured across the transverse or longitudinal directions of a scaffold offers a means to visualize the local number of cells, corresponding to the number of black pixels, throughout (**Figures 5E, F**). Variations in these values represent local variations in the number of cells present. Linear regression analysis is used to fit a straight line to the grayscale distributions as a means to represent the uniformity across the field of view. For a perfectly uniform distribution, linear regression will result in a horizontal line. It's seen that linear regression results in a nearly horizontal line when measured across both the transverse and longitudinal directions (**Figure 5E, F**), indicating a largely uniform distribution of cells throughout the field of view.

The distribution of cells throughout a field of view can also be quantified using particle analysis methods. The uniformity measure *U* (**Equation 1**) is defined using the Shannon entropy of the printed scaffold, $s_{printed}$, Shannon entropy of a perfectly nonuniform particle distribution, $s_{nonuniform}$, and Shannon entropy of a perfectly uniform particle distribution, $s_{uniform}$. Shannon entropy *s* (**Equation 2**) is calculated for a field of view with *N* pixel columns/rows across a field of view based on the probability p_j (**Equation 3**) that a particle lies within the *j*th pixel column/row, where m_j is the grayscale value of the *j*th column/row and *M* is the sum of grayscale values across the field of view. The uniformity value *U* ranges from 0 for a perfectly nonuniform distribution in which cells are present in exactly half of the field of view, to 1 where cells are present exactly equally throughout the full field.

$$U \equiv \frac{s_{printed} - s_{nonuniform}}{s_{uniform} - s_{nonuniform}} \qquad \textbf{Equation 1}$$

$$s = -\sum_j^N p_j \ln p_j \qquad \textbf{Equation 2}$$

$$p_j = \frac{m_j}{M} \qquad \textbf{Equation 3}$$

For the typical field of view shown in **Figure 5A**, uniformity measured across the transverse direction U_{trans} is 0.87, indicating a largely uniform distribution of cells. Uniformity measured across the longitudinal direction U_{long} is 0.95, indicating a distribution even closer to perfectly uniform. Reasoning for the variation in these measures can be visualized in **Figure 5E** and **Figure 5F**. More severe peaks and valleys are present in relative cellularity values measured across the transverse direction when compared to those measured across the longitudinal direction. This can be attributed to cell elongation, which acts to increase the grayscale value in the direction of elongation (pixel columns measured across the transverse direction). Regardless, both measures are indicative of a high uniformity of cells throughout the field of view. Across multiple printed scaffolds with varying cell types and in multiple fields of view, the measured uniformity *U* was greater than 0.8, indicating that CDC fabrication consistently produces uniformly cellularized scaffolds.

The alignment of cells within scaffolds was also quantified for typical scaffold printed with human tenocytes stained and imaged with the cytoplasmic label DiD (green) after 4 days in culture. Directionality analysis of the fiber-only component of using fiber autofluorescence at 405 nm with the peak normalized to 0 degrees shows a narrow frequency distribution, indicating highly parallel fiber with nearly all directional components within 10 degrees of the peak orientation (**Figure 5B**). Similarly, directionality analysis of the cell-only component of the scaffold shows a frequency distribution with a peak orientation identical to the fiber direction, indicating a significant degree of cell alignment and elongation in the direction of the fiber (**Figure 5C**). Across multiple printed scaffolds with varying cell types and in multiple fields of view, a high degree of directionality was measured for fiber and cells, indicating that cells align with the highly parallel fiber.

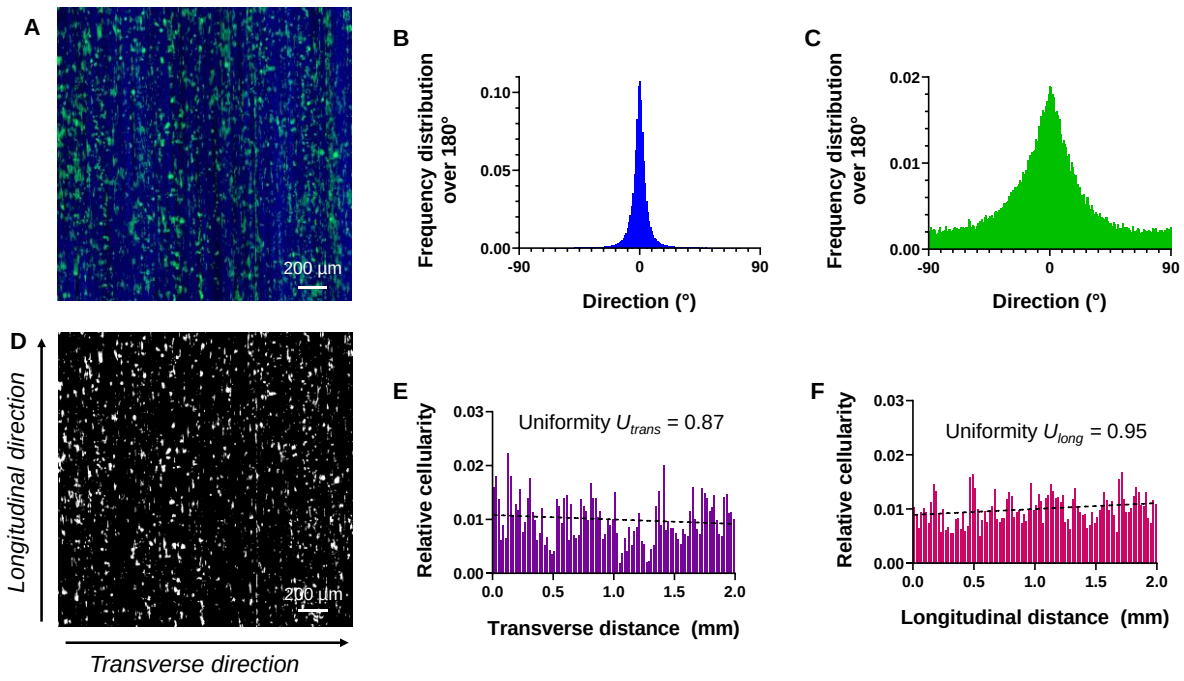

Figure 5. Quantitative cell distribution and alignment. (A) Typical field of view of a printed scaffold with rat muscle progenitor cells distributed throughout and aligned after 14 days in culture. Fluorescence image shows all cells with the cytoplasmic label DiD (green) and collagen fiber autofluorescence at 405 nm (blue). (B) Directionality analysis of the fiber-only component of a typical printed graft, indicating highly parallel fiber. (C) Directionality analysis of the cell-only component of a typical printed graft, indicating a high degree of alignment in the fiber direction. (D) Image shown in A converted to binary for cell distribution analysis with cells indicated in white, background in black, and transverse and longitudinal directions labeled. Relative cellularity plotted along the transverse (E) and longitudinal (F) directions, with nearly horizontal linear regression (dashed lines) and quantified uniformity measure U (ranging from 0 to 1) indicating a highly uniform distribution of cells.

3. Assessment of scaffold mechanical properties

Collagen microfiber scaffolds were printed with and without cells using the CDC fabrication approach and their mechanical properties were assessed. Cellular scaffolds were printed with hMSCs and acellular scaffolds were produced using identical conditions. Scaffolds were tested after 1 day and 28 days in culture and imaged after 1 day and 26 days in culture (**Figure 4A**), closely corresponding to the mechanical testing timepoints. Scaffolds were secured using suture at each end, removed from frames, and returned to culture media the day of testing for scaffolds tested after 1 day of culture and the day prior to testing for scaffolds tested after 28 days of culture.

Scaffolds were mounted to a custom 2-pin setup (**Figure 6A**) on a uniaxial tensile testing machine (MTS Systems Corporation, Eden Prairie, MN) with a 100 N load cell. The 2-pin setup allows for scaffolds secured with suture to be looped around two horizontal steel dowel pins, each of which is mounted to the tensile testing machine such that the distance between the pins increases during testing. This approach was found to provide significantly more consistent results when compared to mounting scaffolds in standard compression grips, which often lead to scaffold damage, slippage, or staggered breakage of individual fibers within a scaffold. Scaffolds were pulled to failure with a pin displacement speed of 1 mm/sec and load and displacement data were recorded. Ultimate tensile stress (UTS) was determined by the peak load and scaffold cross sectional area, and tangent modulus was determined by the slope of the linear region of the stress-strain curve. Strain at break was determined by the initial gauge length and pin displacement at failure. Typical stress-strain curves for each tested group are shown in **Figure 6B**, with distinct "toe" regions of gradually increasing slope followed by linear regions of maximum slope and ultimately sharp well-defined decreases in stress at failure.

Mechanical properties were calculated and reported using two methods for determining the cross-sectional area of printed scaffolds. First, the "solid only" cross-sectional area was determined by multiplying the measured cross-sectional area of individual collagen fibers by the total number of constituent fibers within the printed grafts. The diameter of individual hydrated fibers was measured using microscopic imaging, and the total number of constituent fibers was a controlled user input to the printing process. Second, the "full graft" cross-sectional area was measured manually using digital calipers. Comparing these two methods, mechanical properties determined using the solid only cross section are indicative of the properties of the constituent collagen fiber comprising the grafts, while properties determined using the full graft cross section consider the void space and inherently limited packing density of constituent fiber. Solid only cross-sectional area was assumed to be identical for each experimental group based on the stability of the constituent collagen fiber in culture, and full graft cross-sections were measured for each experimental group immediately prior to testing (**Figure 6C**).

UTS, tangent modulus, and strain at break, are shown in **Figure 6D, E, and F**, respectively, for acellular and cellular scaffolds tested to failure after 1 day and 28 days of culture (n=10 for all groups). For plots displaying UTS (**Figure 6D**) and tangent modulus (**Figure 6E**), horizontal lines are plotted representing the mean UTS and tensile modulus of human ACL (*a)* [Appendix A, journal article], of the strongest portion of the human supraspinatus tendon (*b)* [Appendix B, journal article], and of typical collagen gels used in tissue engineering (*c)* [Appendix C, journal article]. It's seen that depending on the method for determining cross-sectional area, both acellular and cellular scaffolds produced using CDC fabrication nearly match or exceed key mechanical properties of representative native human tendons directly after printing and continue to do so after 28 days in culture. Additionally, the UTS and modulus of collagen microfiber scaffolds produced using CDC fabrication are orders of magnitude larger than the strength and stiffness of collagen gels commonplace in biomanufacturing approaches, which have a typical UTS on the order of 20 kPa and typical tensile modulus on the order of 200 kPa [Appendix C, journal article]. Both acellular and cellular scaffolds after 1 day and 28 days in culture had mean failure strains ranging from 20% to 25% (**Figure 6F**). Unlike UTS and modulus, strain is not dependent on cross-sectional area such that results do not differ when the considering solid only or full graft measurement approaches.

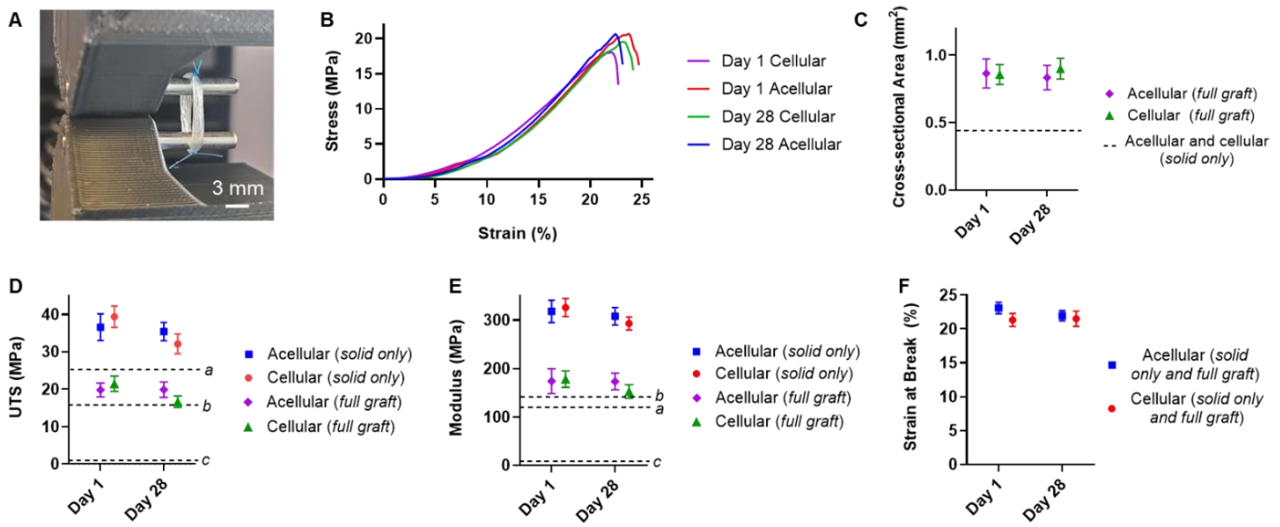

Figure 6. Scaffold mechanical properties. Data obtained from acellular scaffolds (n=10 each time point) and cellular scaffolds (n=10 each time point) containing hMSCs after 1 day and 28 days of culture. Error bars represent standard deviation. (A) 2-pin uniaxial tensile tensing setup offering improved consistency compared to traditional compression grips. (B) Typical stress-strain curves for each experimental group based on the "full graft" with cross-sectional area. (C) Measured full graft and solid only cross-sectional areas. (D) Ultimate tensile stress (UTS). (E) Tangent modulus. (F) Strain at break. [a] Mean UTS and modulus of human ACL [Appendix A, journal article]. [b] Mean UTS and modulus of the strongest portion of the human supraspinatus tendon [Appendix B, journal article]. [c] Mean UTS and modulus of typical collagen gels used in tissue engineering [Appendix C, journal article].

In all, using clinically relevant biomaterials and cells, the novel CDC biofabrication process is capable of printing constructs mimicking some of the biological, morphological, material, and functional properties of native musculoskeletal tissue. Graft geometries are customizable and well-controlled. Cells are found to maintain high viability, proliferate, and elongate with uniform cellular distributions throughout grafts. Graft mechanical properties are found to mimic those of native tissue and exceed the properties achieved by traditional tissue engineering approaches by orders of magnitude.

What opportunities for training and professional development has the project provided?

The project provided several opportunities for training and professional development for primary contributors to the project as well as interns. Researchers gained greater proficiency from interdisciplinary technical training by colleagues from varying backgrounds spanning chemistry, biology, and mechanical/biomedical engineering. Further knowledge and skills were developed by attending conferences and symposiums, both in person (4th Annual Mid-Atlantic Advanced Biomanufacturing Symposium, University of Virginia, VA) and online (AM Medical Virtual Summit and 3DHEALS2020 Virtual Webinar) due to the effects of COVID-19.

How were the results disseminated to communities of interest?

Results achieved from this project were disseminated to the biofabrication community as well as the general public at the 4th Annual Mid-Atlantic Advanced Biomanufacturing Symposium at the University of Virginia, with the poster winning first place in the associated competition. Our work was also submitted and accepted for poster presentation at the Military Health System Research Symposium, which was later canceled due to COVID-19.

What do you plan to do during the next reporting period to accomplish the goals?

1. Produce collagen microfiber grafts with and without hMSCs for bioreactor optimization studies and preliminary rat Achilles-MTJ defect model.

2. Design and modify bioreactor components and process parameters for optimal performance and conduct pilot test.

3. Validate cell labeling on printed grafts to distinguish between intrinsic cells for upcoming rat Achilles-MTJ defect model.

4. **IMPACT:**

What was the impact on the development of the principal discipline(s) of the project?

A novel biomanufacturing, or three-dimensional (3D) bioprinting, approach was developed which offers a significant contribution to the state of the art in tissue engineering technology. This process is capable of producing living tissue-like grafts from strong clinical-grade collagen fibers and human cells. These grafts are made with customized geometries and mimic key biological, material, and functional properties of native musculoskeletal tissue with significant advantages over past tissue engineering approaches. It's envisioned that this platform technology can produce cellularized grafts on-demand which promote regeneration and functional recovery in debilitating musculoskeletal tissue injuries.

What was the impact on other disciplines?

While still in development, the biomanufacturing technology platform and resulting biomimetic grafts prospectively offer the potential to drastically improve the treatment paradigm for musculoskeletal tissue injuries. Foreseeably, the adoption of functional bioprinted grafts by surgeons and care providers eliminates challenges associated with current treatment options and may lead to significantly improved patient outcomes.

What was the impact on technology transfer?

As a biotechnology start-up company, we are currently developing the technology and working toward commercialization. With further development, the technology could foreseeably be adopted by various government or industry biomanufacturing research, development, and manufacturing operations.

What was the impact on society beyond science and technology?

While still requiring significant development and commercialization, biomanufactured grafts prospectively offer next-generation treatments for the millions of Americans suffering musculoskeletal tissue injuries each year. This can translate to significantly improved patient outcomes by accelerating or facilitating the return to activity or even daily life, as well as possible improved efficacy, logistics, and economic benefits to the healthcare system as a whole.

5. CHANGES/PROBLEMS:

Changes in approach and reasons for change

Nothing to report.

Actual or anticipated problems or delays and actions or plans to resolve them

Preliminary animal model-related planning and preparation was delayed due to the effects of the COVID-19 global pandemic. Specifically, collaborating university laboratories were shut down. Efforts to progress toward the rat Achilles-MTJ defect animal model will resume as access to these required facilities becomes available. Depending on the length of closure, we anticipate a delay in completing this animal study.

Changes that had a significant impact on expenditures

The closure of university labs/campuses due to COVID-19 has led to delays in experimental progress and a significantly reduced expenditure from what was projected. While substantial progress was still made regarding technology development, expenditures for the upcoming animal study have been delayed due to the inability access related university facilities. Efforts are being made to resume these studies as soon as possible.

Significant changes in use or care of human subjects, vertebrate animals, biohazards, and/or select agents

Significant changes in use or care of human subjects

Nothing to report.

Significant changes in use or care of vertebrate animals

Nothing to report.

Significant changes in use of biohazards and/or select agents

Nothing to report.

6. PRODUCTS:

- **Publications, conference papers, and presentations**

Journal publications.

Nothing to report.

Books or other non-periodical, one-time publications.

Nothing to report.

Other publications, conference papers and presentations.

Poster presentation at the 4th Annual Mid-Atlantic Advanced Biomanufacturing Symposium at the University of Virginia, VA.

Abstract accepted for poster presentation at the Military Health System Research Symposium, which was later canceled due to COVID-19.

- **Website(s) or other Internet site(s)**

Nothing to report.

- **Technologies or techniques**

A novel biomanufacturing, or three-dimensional (3D) bioprinting, platform technology and related techniques were developed. Currently, the technology and process remain in-house only.

- **Inventions, patent applications, and/or licenses**

Nothing to report.

- **Other Products**

A novel biomanufacturing, or three-dimensional (3D) bioprinting, platform technology and related techniques were developed. It's envisioned that this technology can produce cellularized grafts on-demand which promote regeneration and functional recovery in musculoskeletal tissue injuries.

7. PARTICIPANTS & OTHER COLLABORATING ORGANIZATIONS

What individuals have worked on the project?

Name:	Dr. Michael Francis
Project Role:	Principal Investigator
Researcher Identifier:	991506
Nearest person month worked:	3
Contribution to project:	Project guidance with expertise and emphasis on biological characterization and clinical relevance
Name:	Dr. Kyle Christensen
Project Role:	Postdoctoral Research Associate
Researcher Identifier:	NA
Nearest person month worked:	3
Contribution to project:	Project lead with emphasis and expertise on process design, engineering, and experimental validation

Has there been a change in the active other support of the PD/PI(s) or senior/key personnel since the last reporting period?

Nothing to report.

What other organizations were involved as partners?

Organization Name: Old Dominion University
Location of Organization: Norfolk, VA
Partner's contribution to project: Collaboration on primary project goals, particularly conducting animal studies and related analysis

8. SPECIAL REPORTING REQUIREMENTS

Quad Chart is attached with the submission.

9. APPENDICES:

Three journal articles are attached with the submission as Appendices A, B, and C, and referenced in the text.